Studies on the polycrystalline silicon/SiO_2 stack as front surface field for IBC solar cells by two-dimensional simulations*

Shuai Jiang(姜帅)[1,2,†], Rui Jia(贾锐)[1,‡], Ke Tao(陶科)[1], Caixia Hou(侯彩霞)[1], Hengchao Sun(孙恒超)[1], Zhiyong Yu(于志泳)[3], and Yongtao Li(李勇滔)[1]

[1] *Institute of Microelectronics, Chinese Academy of Sciences, Beijing* 100029, *China*
[2] *University of Chinese Academy of Sciences, Beijing* 100049, *China*
[3] *Jiangxi Science & Technology Normal University, Nanchang* 330013, *China*

(Received 21 March 2017; revised manuscript received 9 May 2017; published online 10 July 2017)

Interdigitated back contact (IBC) solar cells can achieve a very high efficiency due to its less optical losses. But IBC solar cells demand for high quality passivation of the front surface. In this paper, a polycrystalline silicon/SiO_2 stack structure as front surface field to passivate the front surface of IBC solar cells is proposed. The passivation quality of this structure is investigated by two dimensional simulations. Polycrystalline silicon layer and SiO_2 layer are optimized to get the best passivation quality of the IBC solar cell. Simulation results indicate that the doping level of polycrystalline silicon should be high enough to allow a very thin polycrystalline silicon layer to ensure an effective passivation and small optical losses at the same time. The thickness of SiO_2 should be neither too thin nor too thick, and the optimal thickness is 1.2 nm. Furthermore, the lateral transport properties of electrons are investigated, and the simulation results indicate that a high doping level and conductivity of polycrystalline silicon can improve the lateral transportation of electrons and then the cell performance.

Keywords: polycrystalline silicon, SiO_2, solar cell, passivation, simulation, IBC

PACS: 78.56.–a, 77.55.df, 82.20.Wt, 82.45.Bb **DOI:** 10.1088/1674-1056/26/8/087802

1. Introduction

Interdigitated back contact (IBC) solar cells are one of the most efficient solar cells based on silicon.[1] In the IBC solar cells, both the p^+ and n^+ junctions are located on the rear side of the devices. Therefore, there is no metallization pattern on the front surface, which result in very little optical losses and high J_{sc}.[2] In addition, as all metallization patterns are located on rear side, there is no trade-off between series resistance and grid shading, and therefore, the metallization patterns can cover the most rear side of the devices to reduce series resistance and the rear junctions can be optimized in terms of the lowest saturation current only. Furthermore, because the metallization pattern covers most rear side, the lateral current in rear doped region will be avoided, which also contributes to the reduction of internal series resistance.

The industrial manufacturability of IBC solar cells has been demonstrated by many companies and organizations in recent years. SunPower corporation had reported an industrial production of 5-inch (1 inch = 2.54 cm) IBC cells with efficiencies as high as 25%.[3] A 2 cm×2 cm IBC solar cell reported by AUN and trina together achieved a efficiency of 24.6%.[4] IMEC also reported a 2 cm×2 cm IBC with efficiency of 23.1%.[5] Screen-printed technology was used by ISC Konstanz to form contacts for IBC solar cells which achieved a efficiency of 21.3% illustrating the potential of the low-cost approach.[6] The world-record efficiency of silicon solar cell was achieved by Panasonic Corporation in early 2014 by combining interdigitated back contact design and heterojunction structure together.[7]

IBC solar cells have a high quality demand for front surface passivation and bulk minority carrier lifetime, because most electron–hole pairs are generated near front surface and have to diffuse to the rear side to be collected. The requirement of high bulk minority carrier lifetime can be satisfied by using high quality monocrystalline silicon. In order to get a high quality passivation of front surface, lots of methods have been developed. Traditionally, thermal oxide silicon had been applied to effectively passivate the front surface.[8–10] SiN_x is also the most commonly used passivation layer for the front surface of IBC solar cells, and what is more, SiN_x is extremely suitable for antireflective coating because its refractive index is easily adjustable.[11,12] Most recently, some researchers used

*Project supported by the National Natural Science Foundation of China (Grant Nos. 11104319, 11274346, 51202285, 61234005, 51172268, 51602340, 61274059, and 51402347), the Solar Energy Action Plan of Chinese Academy of Sciences (Grant Nos. Y1YT064001, Y1YF034001, and Y2YF014001), the Graduate and College Student's Innovative Project (Grant No. YC2016-X19), the Project of Beijing Municipal Science and Technology Commission (Grant No. Z151100003515003), and the Opening Project of Key Laboratory of Microelectronics Devices & Integrated Technology, Institute of Microelectronics, Chinese Academy of Sciences.

†Corresponding author. E-mail: jiangshuai@ime.ac.cn
‡Corresponding author. E-mail: jiarui_solar@souhu.com

© 2017 Chinese Physical Society and IOP Publishing Ltd

aluminium oxide (Al_2O_3) as passivation layer and obtained a good result due to its low density of the interface defects.[13] In addition, amorphous silicon (a-Si) and SiO_2/SiN_x stack had also been demonstrated by many researchers to be good passivation material.[14]

All the passivation methods mentioned above passivate silicon surface by reducing dangling bonds on surface of silicon substrate which is called chemical-effect passivation. There is another kind of passivation technique called field-effect passivation which apply an electric field near the surface to reduce the concentration of one type of carriers. The electric field can be generated by forming a high-low junction[15] or a PN junction[16] near the surface. Most current IBC solar cell's front surface are passivated by applying those two methods at the same time.

In the present work, we propose a new approach to combine the chemical passivation and field passivation together to passivate the front surface of the IBC solar cells. To be specific, the passivation structure includes a highly doped polycrystalline silicon layer and a thin SiO_2 layer. The SiO_2 is inserted between polycrystalline silicon layer and c-Si substrate. This SiO_2 layer can effectively reduce dangling bonds at the surface of c-Si substrate to provide a high quality of chemical passivation. The highly doped polycrystalline silicon is used to form a heterojunction with the moderately doped substrate to provide a high quality of field passivation. In this paper, we investigated the properties of the polycrystalline silicon/SiO_2 stack as front surface field (FSF) of the IBC solar cells only by simulations, but our preliminary experiments on such stack have shown promising results in the passivation of crystalline silicon wafers. Minority carrier lifetime of more than 3 ms indicated the excellent surface passivation capability of this FSF structure. In our simulations, the doping level and thickness of polycrystalline silicon and the thickness of SiO_2 is optimized. Furthermore, the lateral transport properties of electrons in the IBC solar cells with the polycrystalline silicon/SiO_2 stack are investigated too.

2. Simulation method

All the simulations are performed in two dimensions which is necessary for the simulations of IBC solar cells. The parameters used for simulations are listed in Table 1. The TCAD tools we used are the commercial device simulation package which is very good at two-dimensional (2D) devices simulation.

The cross-section of the IBC solar cell structure used in our simulations is shown in Fig. 1. The base of the device is made of monocrystalline silicon whose thickness is 230 μm. On the front surface of the device, SiO_2 layer and polycrystalline silicon layer are deposited successively. On the rear side, selective doped region of P^+ emitter and N^+ back surface field (BSF) is formed and they are separated by a gap region which has the same doping level with the substrate. The doping profile of both P^+ emitter and N^+ BSF conforms to Gaussian distribution with doping peak at the rear surface of substrate. The anode and cathode are formed on the surface of P^+ emitter and N^+ BSF respectively and the whole regions of P^+ emitter and N^+ BSF are covered by electrode contacts. Both anode and cathode are formed by aluminum contacts. Table 1 lists the main reference cell parameters.

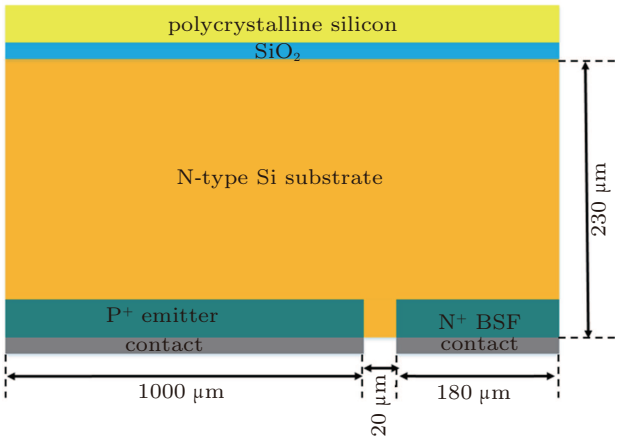


Fig. 1. (color online) The cross-section of IBC solar cell structure used in simulations.

Luminous is a general purpose light propagation and absorption program integrated into the Atlas framework which can calculate optical intensity profiles within the semiconductor devices and then convert the intensity profiles into photo-generation rates which are directly integrated into the generation terms in the carrier continuity equations. This unique coupling of tools can simulate electronic responses to optical signals for a broad range of optical devices. In this method, the photo-generation rate in semiconductor is given by the formula:

$$G = \eta_0 \frac{P\lambda}{hc} \alpha \, \mathrm{e}^{-\alpha y}, \tag{1}$$

where P is the ray intensity factor, η_0 is the internal quantum efficiency, y is a relative distance for the ray, h is Planck's constant, λ is the wavelength, c is the speed of light, and α is the absorption coefficient which equal to $(4\pi/\lambda)k$. Furthermore, the photocurrent can be calculated by the formula:

$$I_{\mathrm{A}} = \eta_0 \frac{B_{\mathrm{n}}\lambda}{hc} \sum_{i=1}^{N_{\mathrm{R}}} W_{\mathrm{R}} \int_0^{Y_i} P_i \alpha_i \, \mathrm{e}^{-\alpha y} \, \mathrm{d}y, \tag{2}$$

where η_0 is the internal quantum efficiency, B_{n} is the intensity of the beam number n, λ is the wavelength, h is Planck's constant, c is the speed of light, N_{R} is the sum of the number of rays traced, W_{R} is the width associated with the ray, P_{i} accounts for the attenuation of the ray and α_i is the absorption coefficient. The integral is taken over the length, Y_i, associated with the ray.

Table 1. Parameters used for the simulated IBC solar cells.

Parameter	Value
Base	
Thickness/μm	230
Type	N
Resistivity/Ω·cm	1.5
mid-gap SRH lifetimes $\tau_n = \tau_p$/μs	3000
SiO_2 layer	
Thickness/nm	0.2∼10
Dielectric constant	3.9
Polycrystalline silicon	
E_g/eV	1.08
Type	N
Doping (N_D)/cm^{-3}	$1\times10^{15}\sim5\times10^{21}$
Thickness/nm	$1\sim20$
Affinity/eV	4.17
Dielectric constant	11.8
Imaginary part of refractive index	2.1
BSF	
Doping (N_D)/cm^{-3}	8×10^{19}
Profile	ERFC
Junction depth/μm	1.5
Surface SRH	
Passivated ($S_p = S_n$)/(cm/s)	1×10^{6}
Contacted ($S_p = S_n$)/(cm/s)	1×10^{7}
Emitter	
Doping (N_A)/cm^{-3}	5.6×10^{19}
Profile	ERFC
Junction depth/μm	0.6
Surface SRH	
Passivated ($S_p = S_n$)/(cm/s)	6850
Contacted ($S_p = S_n$)/(cm/s)	1×10^{7}
Optical confinement	
Reflectivity of front surface of polycrystalline silicon	0.9
Reflectivity of the interface between polycrystalline silicon and SiO_2	0.95
Reflectivity of the interface between SiO_2 and substrate	0.95
Back reflectivity	0.9
Recombination velocity	
Front surface of polycrystalline silicon/(cm/s)	200
The interface between polycrystalline silicon and SiO_2/(cm/s)	200
The interface between SiO_2 and substrate/(cm/s)	100
Spacing between BSF and emitter/μm	20

There are two recombination mechanisms in our simulations. The first one is the Shockley–Read–Hall (SRH) recombination which is dominated in the moderately doped region and surface. The Shockley–Read–Hall (SRH) recombination model can be determined to be concentration-independent or concentration-dependent. We chose the latter model by which the recombination rate is given by the formula[17–19]

$$R_{\mathrm{SRH}} = \frac{pn - n_i^2}{\tau_p\left[n + n_i\exp\left(\frac{E_{\mathrm{TRAP}}}{kT_L}\right)\right] + \tau_n\left[p + n_i\exp\left(\frac{-E_{\mathrm{TRAP}}}{kT_L}\right)\right]}, \tag{3}$$

where

$$\tau_n = \frac{TAUN0}{1 + N_{\mathrm{Dtotal}}5\times10^{16}}, \tag{4}$$

$$\tau_p = \frac{TAUP0}{1 + N_{\mathrm{Dtotal}}5\times10^{16}}, \tag{5}$$

Here, N_{Dtotal} is the total concentration of donors, N_{Atotal} is the total concentration of acceptors, $TAUN0$ and $TAUP0$ is the lifetime of electrons and hole, E_{TRAP} is the trap level energy with respect to Fermi level, n_i is the intrinsic carrier concentration, k is the Boltzmann constant, and T_L is the absolute temperature.

The other recombination mechanism is Auger recombination which is dominated in heavily doped region. The Auger recombination rate is given by the formula[20]

$$R_{\mathrm{Auger}} = AUGN(pn^2 - nn_i^2) + AUGP(np^2 - pn_i^2), \tag{6}$$

where p and n is concentration of holes and electrons, n_i is the intrinsic carrier concentration, $AUGN = 2.8\times10^{-31}$ cm^6/s and $AUGP = 9.9\times10^{-32}$ cm^6/s are the Auger coefficients for electron and hole respectively.

Non-local band to band tunneling model is used to simulate the tunneling of carriers through the SiO_2 layer between polycrystalline silicon layer and substrate. The tunneling probability is given by

$$T(E) = \exp\left(-2\int_{x_{\mathrm{start}}}^{x_{\mathrm{end}}} k(x)\,\mathrm{d}x\right), \tag{7}$$

where

$$k(x) = \frac{k_e k_h}{\sqrt{k_e^2 + k_h^2}}, \tag{8}$$

with

$$k_e(x) = \frac{1}{\mathrm{i}\hbar}\sqrt{2m_0m_e(E - E_c(x))}, \tag{9}$$

and

$$k_h(x) = \frac{1}{\mathrm{i}\hbar}\sqrt{(2m_0m_h(E_v(x) - E))}, \tag{10}$$

where m_0 is the inertia mass of electron, m_e and m_h are the effective mass of electron and hole. $E - E_c(x)$ equals the energy of the potential barrier that electron tunnels through. $E_v(x) - E$ equals the energy of the potential barrier that hole tunnels through. The x_{start} and x_{end} is the start point and end point of the tunneling path.

In addition, the bandgap narrowing effect, concentration dependent mobility, the Fermi–Dirac carrier statistics are considered in our simulations in order to make the simulations more accurate.[20] An AM 1.5G solar spectrum is used for the optical generation to simulate the J–V curve under standard one-sun illumination condition at an intensity of 100 mW·cm^2.

3. Results and discussion

3.1. Passivation of the front surface

3.1.1. The optimization of polycrystalline silicon layer

Firstly, the influence of doping level, varying from 1×10^{15} cm^{-3} to 5×10^{21} cm^{-3}, of polycrystalline silicon with

different thickness (5 nm, 10 nm, 15 nm, 20 nm) on the efficiency of IBC solar cellwas simulated systematically.

Figure 2 shows how the doping level of polycrystalline silicon with different thickness affects the efficiency of IBC solar cells. It can be clearly seen that the efficiency rapidly increases when doping level exceeds 1×10^{16} cm^{-3}, and when doping level exceeds 1×10^{18} cm^{-3}, efficiency increases slowly as doping level further increases.

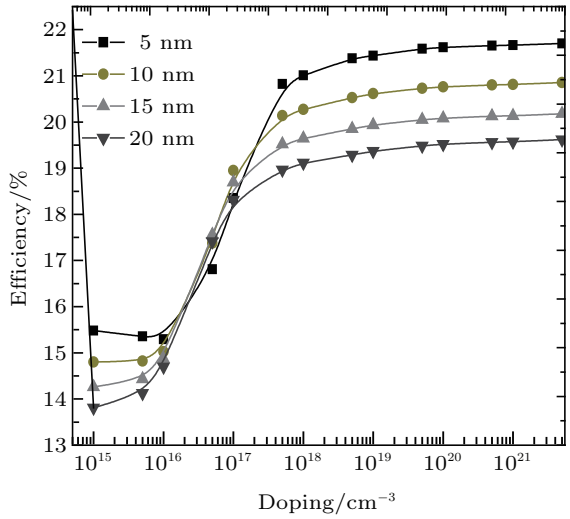


Fig. 2. The efficiency versus doping level of polycrystalline silicon layer with different thickness.

To explain this phenomenon, we compared this structure to the conventional passivation method for front surface field namely FSF. The conventional FSF structure is usually formed by thermal diffusion by which a heavily doped region having the same dopant type with substrate is formed near front surface. Due to different doping level, a high-low junction is formed between the heavily doped region and moderately doped substrate with a vertical build-in electric field pointing from front surface to substrate serving to repel holes and draw electrons to the front surface. In this way, electrons and holes are separated and recombination becomes very low. Similar to the conventional FSF structure, there is also a build-in electric field in the polycrystalline silicon/SiO_2 stack serving to separate holes and electrons to reduce recombination, but instead of a high-low junction, the build-in electric field is formed in a heterojunction. This heterojunction is formed by depositing a thin SiO_2 layer and a heavily doped polycrystalline silicon layer on moderately doped c-Si substrate successively. Once polycrystalline silicon and SiO_2 is deposited on the substrate surface, carriers including holes and electrons will tunnel from the low concentration region through the SiO_2 layer to the high concentration region. Due to carriers transportation, there occur net charges in polycrystalline silicon layer and substrate with opposite polarity, and at the same time, a build-in electric field pointing from front surface to substrate is formed. This build-in field will repel holes away from the front surface to avoid a high recombination of carriers because of the high defect concentration at front surface.

It is obvious that the stronger the electric field is, the smaller the recombination will become. Therefore, it is important to find the parameters that can influence the electric field noticeably. By two dimensional simulations, we find that the doping level of polycrystalline silicon can influence the electric field significantly. In Fig. 3, the electric field intensity near front surface with different doping level of polycrystalline silicon distinguished by different color is shown. The position of 0.01 μm corresponds to the interface between polycrystalline silicon and SiO_2 layer. It can be clearly seen that there is a stronger electric field in both regions of polycrystalline silicon and substrate when doping level of polycrystalline silicon becomes higher. This stronger electric field can be attributed to the higher charge concentration in the heterojunction.

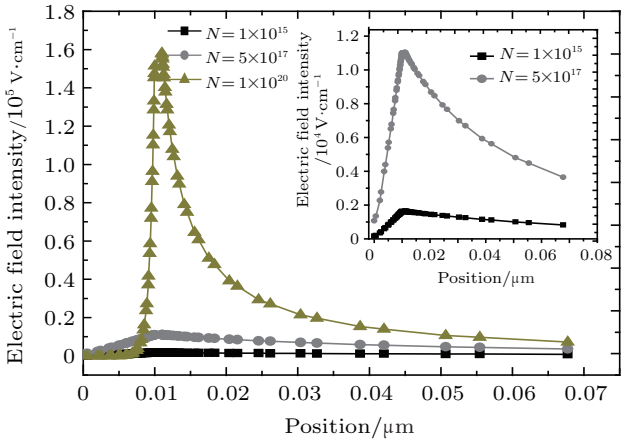


Fig. 3. (color online) The electric field intensity in Y direction near front surface with different doping level of polycrystalline silicon layer. The position of 0.01 μm corresponds to the interface between polycrystalline silicon and SiO_2 layer. The thickness of the polycrystalline silicon layer and SiO_2 layer are 10 nm and 1 nm respectively.

In Fig. 4, the distribution of charges is shown by different colors, while the hole current densities are represented by different arrows whose direction and length symbolizing the direction and magnitudes of the hole current. As can be seen from Fig. 5(a) in which doping level of polycrystalline silicon is 1×10^{15} cm^{-3}, there are nearly no net charges in both polycrystalline silicon and substrate near the interface with SiO_2, and holes in substrate flow towards front surface. The hole current direction in substrate indicates that the electric field is not strong enough to repel holes, and therefore, holes flow toward to front surface because of the high recombination rate at front surface. In contrast, in Fig. 5(b), when polycrystalline silicon's doping level is 1×10^{20}cm^{-3}, there are plenty of net charges in both polycrystalline silicon and substrate,particularly in polycrystalline silicon, near the interface with SiO_2, and holes in substrate flow away from front surface. The holes current direction in substrate indicates that the electric field is strong

enough to compete with the diffusion of holes caused by uneven distribution to repel holes away from front surface, thus keeping holes concentration near font surface at a very low level. Figure 6 shows the holes distribution near front surface with different doping level of polycrystalline silicon which is in line with our analysis above.

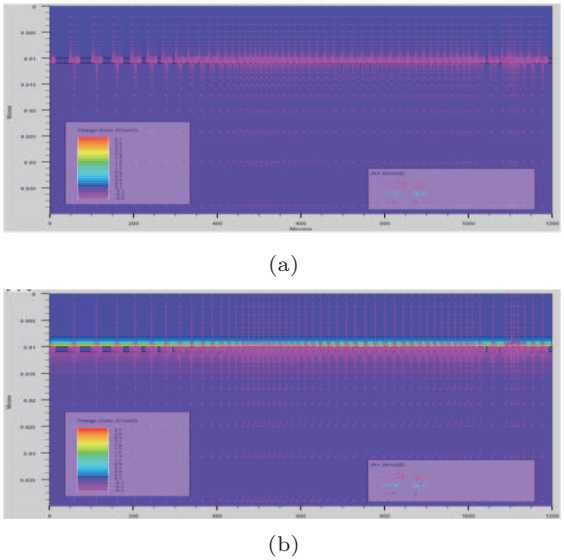


Fig. 4. (color online) The charge distribution and holes current distribution near front surface with polycrystalline siliconlayer's doping level of 10^{17} cm^{-3} (a), and 10^{20} cm^{-3} (b).

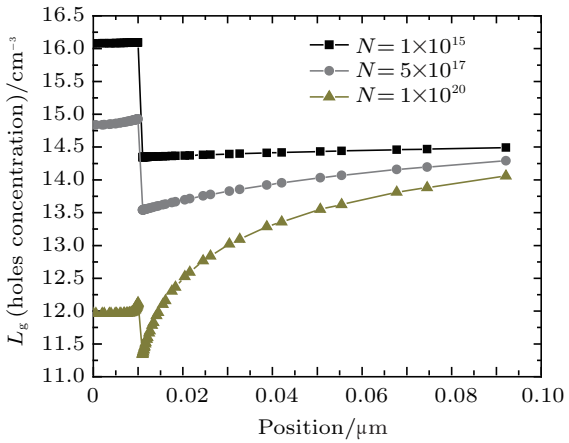


Fig. 5. (color online) The holes concentration near front surface with different doping levels of polycrystalline silicon layer. The position of 0.01 μm corresponds to the interface between polycrystalline silicon layer and SiO_2 layer. The thickness of the polycrystalline silicon layer and SiO_2 layer are 10 nm and 1 nm respectively.

From Fig. 2, we can also find that the thickness of polycrystalline silicon can influence the efficiency of IBC solar cells, and the influence is different while the doping level of polycrystalline silicon changes. Hence the influence of thickness, varying from 1 nm to 20 nm, of polycrystalline silicon with different doping level (1×10^{15} cm^{-3}, 5×10^{17} cm^{-3}, 1×10^{20} cm^{-3}) on solar cell efficiency is simulated.

Figure 6 shows that solar cell efficiency decreases gradually as polycrystalline silicon thickness increases from 1 nm to 20 nm when the doping level of polycrystalline silicon is 1×10^{15} cm^{-3} and 1×10^{20} cm^{-3}, but when the doping level of polycrystalline silicon is 5×10^{17} cm^{-3}, solar cell efficiency shows an increasing tendency as polycrystalline silicon thickness increases from 1 nm to 9 nm, then efficiency decreases gradually as polycrystalline silicon thickness further increases. The different change trends of efficiency indicates that polycrystalline silicon thickness can influence solar cell efficiency in two different ways.

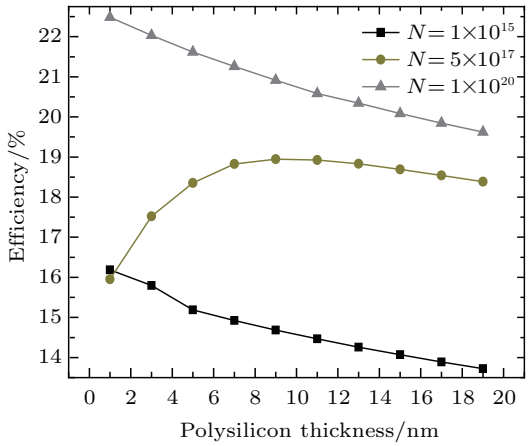


Fig. 6. (color online) The efficiency versus polycrystalline silicon thickness with different doping levels of polycrystalline silicon layer.

Firstly, when polycrystalline silicon thickness increases, more incident light will be absorbed by this polycrystalline silicon layer which can greatly decrease solar cell efficiency. That is why solar cell efficiency decreases markedly as polycrystalline silicon thickness increases when polycrystalline silicon's doping level is 1×10^{15} cm^{-3} and 1×10^{20} cm^{-3}. This assumption can be proved by Fig. 7 in which the external quantum efficiency (EQE) with different polycrystalline silicon thickness is shown. As illustrated in Fig. 7, the EQE decreases as polycrystalline silicon thickness increases, which indicates more optical losses caused by light absorption in polycrystalline silicon.

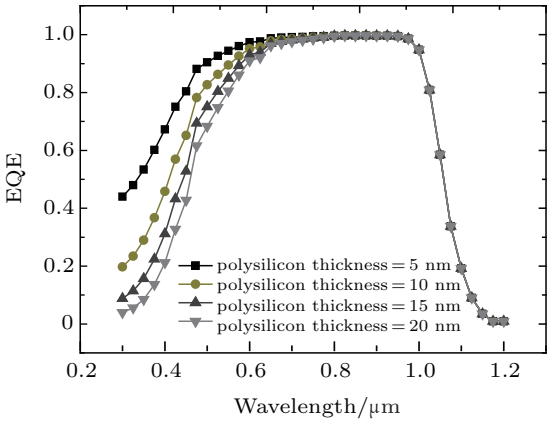


Fig. 7. (color online) The external quantum efficiency (EQE) of solar cells with polycrystalline silicon having different thicknesses and constant doping level of 1×10^{20} cm^{-3}.

To explain the increase trend of efficiency when doping level of polycrystalline silicon is 5×10^{17} cm^{-3}, we find that

the thickness of polycrystalline silicon can also influence the build-in electric field and the influence extent changes with different doping levels of polycrystalline silicon. To make this effect more clear,the charge concentration and electric field intensity near front surface with different polycrystalline silicon thicknesses (3 nm, 9 nm, 19 nm) and different doping levels of polycrystalline silicon (1×10^{15} cm^{-3}, 5×10^{17} cm^{-3}, 1×10^{20} cm^{-3}) are shown in Fig. 8. The doping levels of polycrystalline silicon is 1×10^{15} cm^{-3} in Figs. 8(a) and 8(b), 5×10^{17} cm^{-3} in Figs. 8(c) and 8(d), and 1×10^{20} cm^{-3} in Figs. 8(e) and 8(f). It can be clearly seen that when doping level of polycrystalline silicon is 1×10^{15} cm^{-3} and 1×10^{20} cm^{-3}, the charge concentration at the substrate side and the electric field almost cannot be influenced by polycrystalline silicon thickness. However, when doping level of polycrystalline silicon is 5×10^{17} cm^{-3}, the charge concentration and electric field increase markedly as polycrystalline silicon thickness increases. The reason why the charge concentration and electric field increases as polycrystalline silicon thickness increaseswith doping level of polycrystalline silicon being 5×10^{17} cm^{-3} is that the theoretical width of space charge region at polycrystalline silicon side will exceed the whole width of the polycrystalline silicon layer, and therefore, increasing polycrystalline silicon thickness will add more charges in space charge region and then make the build-in electric field stronger. In contrast, when doping level of polycrystalline silicon is 1×10^{20} cm^{-3}, the theoretical width of space charge region at polycrystalline silicon side is smaller than all the polycrystalline silicon thickness employed in our simulations,

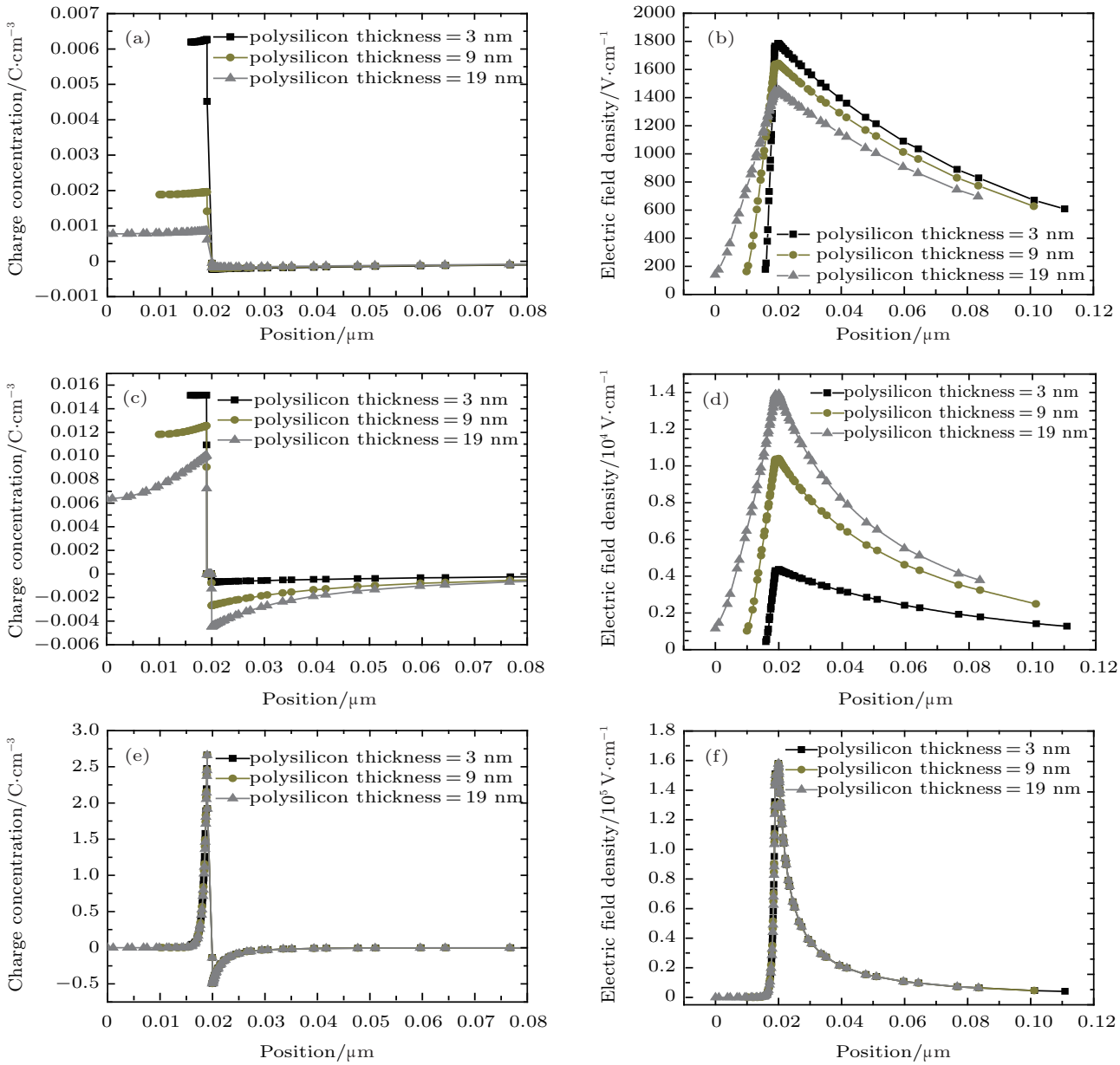


Fig. 8. (color online) The charge concentration and electric field density near front surface with different polycrystalline silicon thicknesses (3 nm, 9 nm, 19 nm) and different polycrystalline silicon doping levels of 1×10^{15} cm^{-3}, (a) and (b); 5×10^{17} cm^{-3}, (c) and (d); 1×10^{20} cm^{-3}, (e) and (f). The position of 0.02 μm corresponds to the interface of polycrystalline silicon and SiO_2, and the thickness of SiO_2 layer is 1 nm.

and therefore, increasing polycrystalline silicon thickness will not add any more charges in space charge region. When doping level of polycrystalline silicon is 1×10^{15} cm^{-3}, the charge concentration in space charge region is very small, although increasing polycrystalline silicon thickness will still add more charges in space charge region, it won't make much difference.

3.1.2. The optimization of silicon oxide layer

In the polycrystalline silicon/SiO_2 stack structure used in this paper, the thin SiO_2 is employed to reduce dangling bonds on the surface of c-Si substrate and then impede the recombination of photon-generated carriers near front surface. Although SiO_2 layer is used mainly for chemical passivation, its thickness can also influence the effect of field passivation. Hence a series of thickness, varying from 0.2 nm to 10 nm, of SiO_2 layer with polycrystalline silicon's doping level of 1×10^{20} cm^{-3} is simulated.

As is presented in Fig. 9, solar cell efficiency sharply increases when SiO_2 thickness increases from 0.2 nm to 1.2 nm. The efficiency then decreases as SiO_2 thickness increases further. The increase trend of efficiency can be explained by considering the recombination of carriers in polycrystalline silicon layer. When the thickness of SiO_2 layer is small enough, the tunneling of electrons through SiO_2 layer becomes very large, a considerably high proportion of electrons are drawn into the polycrystalline silicon layer. In contrast to c-Si substrate, high doping level polycrystalline silicon is a highly defective layer. The SRH recombination is the dominant recombination mechanism in material with a high density of states presenting within band gap. According to the Eq. (3), it is clear that the defects within polycrystalline silicon layer must induce serious recombination losses.

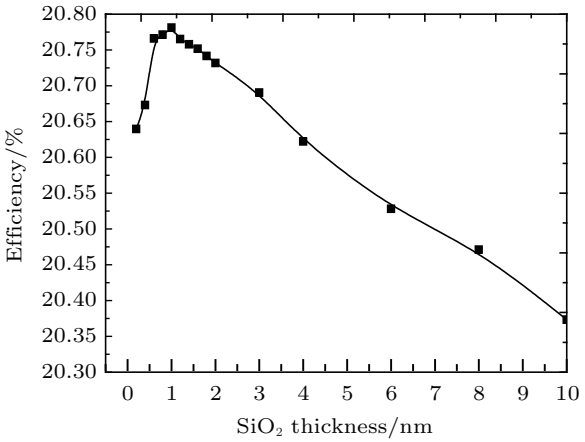


Fig. 9. The efficiency versus SiO_2 thickness with polycrystalline silicon's doping level of 1×10^{20} cm^{-3}.

Figure 10 shows the recombination rate in polycrystalline silicon with different SiO_2 thickness. The position of 10nm corresponds to the interface between polycrystalline silicon layer and SiO_2 layer. It is obvious that the recombination near the interface becomes more serious when SiO_2 layer get thinner.

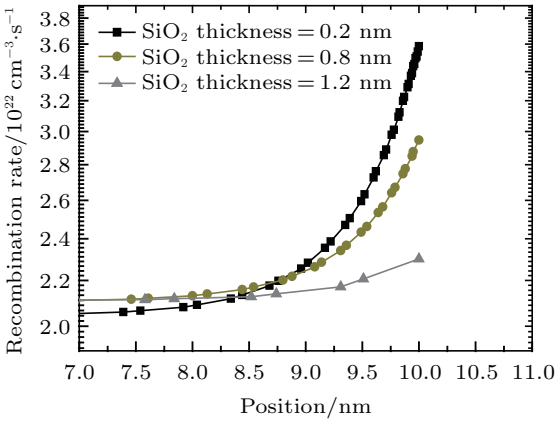


Fig. 10. (color online) The recombination rate at the polycrystalline silicon side near the interface between polycrystalline silicon layer and SiO_2 layer with different SiO_2 thickness. The doping level of polycrystalline silicon is 1×10^{20} cm^{-3} and the thickness of polycrystalline silicon is 10 nm.

The decrease trend of efficiency as SiO_2 thickness further increases can be attributed to the weakening of electric field near the interface between substrate and SiO_2 layer as SiO_2 layer thickness increases. In Fig. 11, the electric field intensity near front surface is shown. To make the comparison more clear, the region of SiO_2 is not shown in the graph, which won't cause any inaccuracy because the electric field in SiO_2 is constant. By comparison, it can be clearly seen that electric field dramatically decreases when the thickness of SiO_2 increases. To further explain this effect, the electrical potential near front surface is shown in Fig. 12, the vertical line with different colors corresponds to the interface between SiO_2 layer and substrate. It can be seen that the potential barrier from the deep of substrate to the interface increases as SiO_2 thickness decreases. This is because the thicker the SiO_2 layer is, the more potential will drop in SiO_2 layer. A higher potential barrier means thatit's harder for holes to reach the interface and the hole concentration will become lower as shown in Fig. 13.

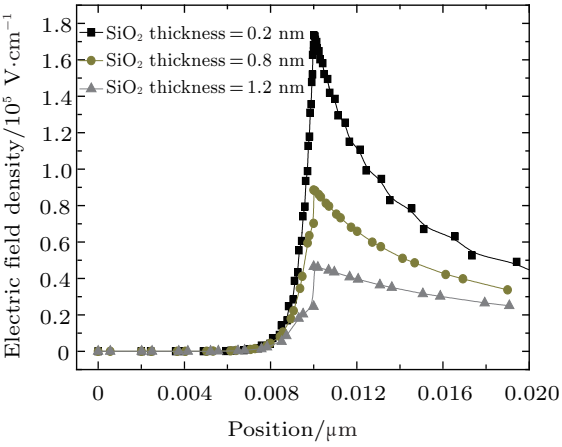


Fig. 11. (color online) The electric field density near front surface with different thicknesses of SiO_2 layer. The position of 0.01 μm corresponds to the interface between polycrystalline silicon and SiO_2. The region of SiO_2 layer is omitted in the graph since the electric field in SiO_2 layer is constant.

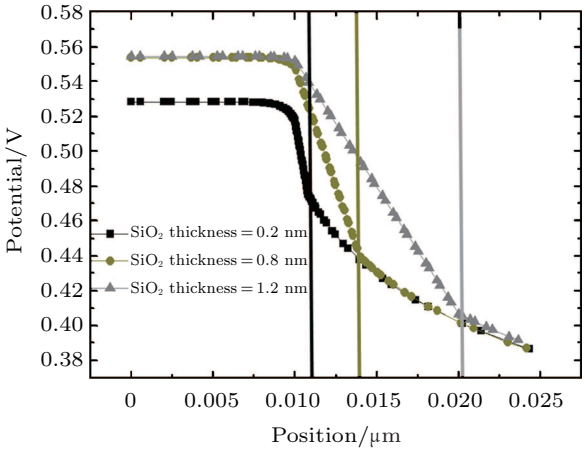


Fig. 12. (color online) The potential near front surface with different SiO_2 layer thicknesses. The vertical line in graph denote the interface between SiO_2 layer and substrate.

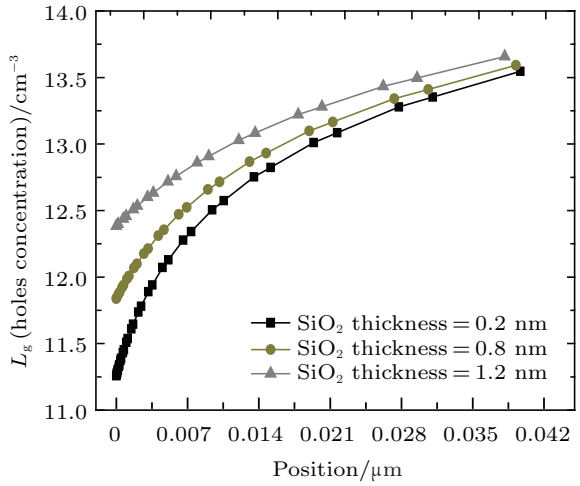


Fig. 13. (color online) The hole concentration at the substrate side near the interface between substrate and SiO_2 layer with different SiO_2 thicknesses. The position of 0 μm corresponds to the interface between substrate and SiO_2 layer.

3.2. The lateral transport properties of electrons

Lateral transportation of carriers in IBC solar cell is very important because in order to allow all contacts to be applied on rear side, the rear colleting junction (the emitter) is interrupted by a non-collecting junction (the BSF).[18] Therefore, any carriers that are generated above a BSF area need to travel laterally to an emitter area. A high lateral conductivity is beneficial to the lateral transportation of carriers and then the solar cell performance. In order to investigate the influence of the polycrystalline silicon/SiO_2 stack on solar cell performance, the influence of polycrystalline silicon's doping level and thickness on fill factor which is directly related to the lateral transportation of carriers is simulated, and the results are presented in Fig. 14. As is illustrated in Fig. 14, the fill factor keep increasing as doping level of polycrystalline silicon vary from 1×10^{15} cm^{-3} to 5×10^{21} cm^{-3} for all investigated polycrystalline silicon layer thicknesses.

We attributed this effect to the accumulation of electrons near front surface caused by the build-in electric field. As discussed above, there is a build-in electric field in the heterojunction which can repel holes away from front surface. Except for that, this build-in electric field can draw electrons towards front surface, which result in a region where electron concentration is extremely high. As electrons accumulate in this region, the conductivity of this accumulation layer increases. According to the basic laws of circuit, current tend to flow through high conductivity path, therefore, a great portion of electron current will flow through the accumulation layer near front surface. Figure 15 shows the electron current density near the interface between substrate and SiO_2 layer with different doping levels of polycrystalline silicon. It can be seen that almost all the electron current gather in an arrow region near front surface. As is also presented in Fig. 15, the electron current increase dramatically as doping level of polycrystalline silicon increases. This is reasonable because higher doping level of polycrystalline silicon will lead to a stronger build-in electric field, and therefore, more electrons will be drawn to front surface resulting in a more conductive layer and larger electron current.

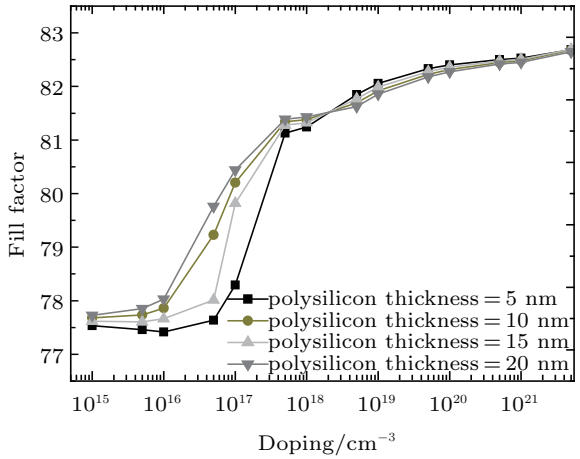


Fig. 14. (color online) The fill factor of IBC solar cells versus doping level of polycrystalline silicon with different polycrystalline silicon thicknesses.

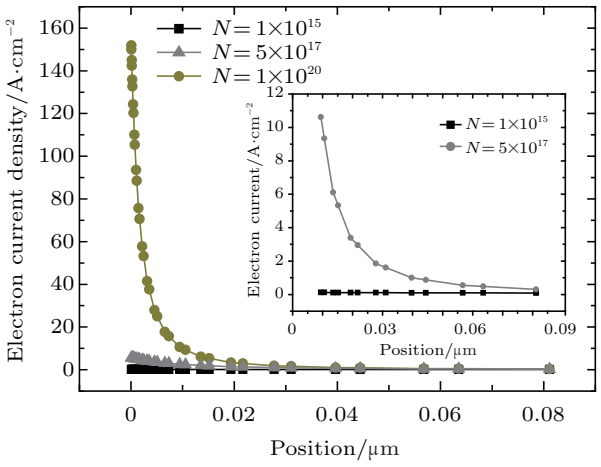


Fig. 15. (color online) The electron current density on the substrate side near the interface between substrate and SiO_2 layer with different doping levels of polycrystalline silicon.

As discussed in Subsubsection 3.1.2, when the build-in electric field is strong enough and SiO_2 layer is thin enough, a portion of electron will be draw into the polycrystalline silicon layer through SiO_2 layer by tunneling. So, it's reasonable to speculate that a portion of electron current will also be draw into polycrystalline silicon layer which can influence the lateral transport properties of electrons and then the fill factor of IBC solar cell.

To see if there is electron current in the polycrystalline silicon layer, the electron current density near front surface with different doping level of polycrystalline silicon is presented in Fig. 16. In Fig. 16, the direction and length of the arrows symbolizing the direction and magnitudes of total electron current. As is presented in Fig. 16(a), when the doping level of polycrystalline silicon is 1×10^{15} cm^{-3}, there is almost no electron current flowing in polycrystalline silicon layer. However, when the doping level of polycrystalline silicon increases to 1×10^{20} cm^{-3}, a great deal of electron current flow through polycrystalline silicon layer as is shown in Fig. 16(c).

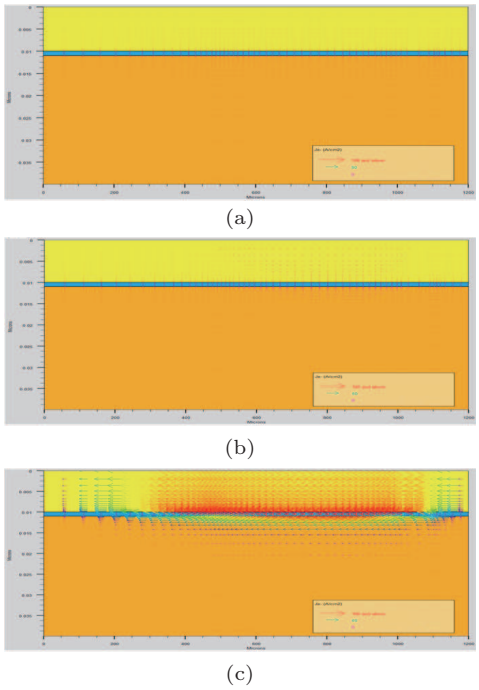


Fig. 16. (color online) The electron current distribution near front surface with different polycrystalline silicon's doping level of 1×10^{15} cm^{-3}, (a), 5×10^{17} cm^{-3}, (b), 1×10^{20} cm^{-3}, (c).

The electron current in polycrystalline silicon layer is not a full condition to improve the lateral transport properties of IBC solar. In order to make the photo-generated carriers to be collected by emitter and BSF, there must be an influent and effluent electron current at the interface between polycrystalline silicon and SiO_2 at the same time. To see if there are an influent and effluent electron current at the same time, the electron current density in Y direction at the interface between polycrystalline silicon and SiO_2 with different doping level of polycrystalline silicon is plotted in Fig. 17. The width in X direction covers a whole pitch of IBC solar cell which including both emit and BSF. It can be clearly seen that there is only positive current which indicate an effluent electron current in the whole range of a pitch when doping level of polycrystalline silicon is 1×10^{15} cm^{-3} and 5×10^{17} cm^{-3}. In contrast, when doping level of polycrystalline silicon is 1×10^{20} cm^{-3}, there are both positive and negtive current in the whole range of a pitch, which indicates both influent and effluent electron current at the same time.

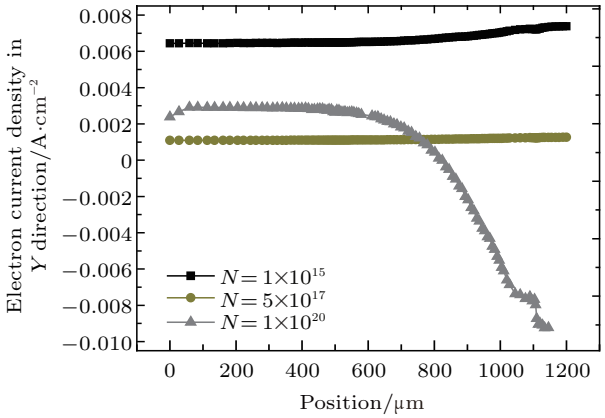


Fig. 17. (color online) The electron current density in Y direction at the interface between polycrystalline silicon and SiO_2 with different doping levels of polycrystalline silicon layer. The range of X axis covers a whole pitch of the IBC solar cell.

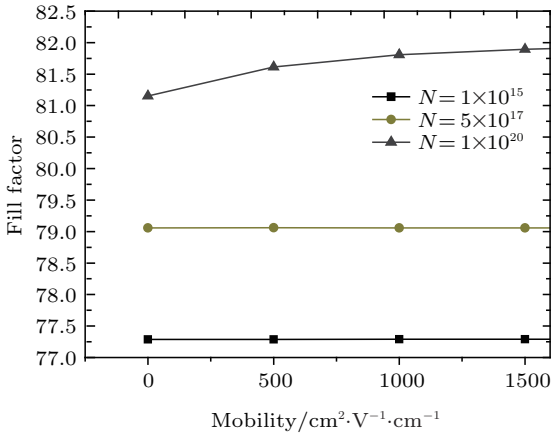


Fig. 18. (color online) The fill factor of IBC solar cells versus the mobility of polycrystalline silicon with different doping levels.

To relate this effect directly to the performance of IBC solar cells, we change the mobility of polycrystalline silicon layer while keeping the doping level invariant to investigate the influence of electron current in polycrystalline silicon layer on the fill factor of IBC solar cells. As shown in Fig. 18, fill factor does not change as mobility increases when doping level of polycrystalline silicon is 1×10^{15} cm^{-3} and 5×10^{17} cm^{-3}, which is in good agreement with the analysis above that electron current in polycrystalline silicon layer has no influence on lateral transport properties when doping level of polycrystalline silicon is 1×10^{15} cm^{-3} and 5×10^{17} cm^{-3}. In con-

trast, the fill factor increases as mobility increases when doping level of polycrystalline silicon is 1×10^{20} cm^{-3}, and therefore, a good conductivity of polycrystalline silicon layer is good for the performance of IBC solar cell in this doping level.

4. Conclusion

The polycrystalline silicon/SiO_2 stack cannot only efficiently passivate the front surface of IBC solar cellsbut also improve the lateral transport properties of electrons, which ensures a high conversion efficiency. Simulations have been done to optimize the polycrystalline silicon layer and SiO_2 layer to achieve the best performance of IBC solar cells. The simulation results show that both the thickness and doping level of polycrystalline silicon can influence the passivation effect of the front surface of IBC solar cells. If the doping level of polycrystalline silicon is not high enough, the thicker the polycrystalline silicon layer is, the better passivation effect can be achieved. However, if doping level of polycrystalline silicon is high enough, the thickness of polycrystalline silicon can hardly affect the passivation quality of front surface. On the other hand, a thicker polycrystalline silicon layer will cause more optical losses, and therefore, the polycrystalline silicon layer should be as thin as possible. Hence the doping level should be high enough to allow a very thin polycrystalline silicon layer to ensure an effective passivation and very small optical losses at the same time.The results of the optimization for SiO_2 layer indicate that SiO_2 should neither be too thin or too thick. The optimal thickness of SiO_2 is 1.2 nm.In addition, the lateral transport properties of electrons were simulated. The results indicate that increasing the doping level of polycrystalline silicon will improve the lateral transportation of electrons. What is more, we find that a portion of electron current will be drawn into the polycrystalline silicon layer when the doping level of polycrystalline silicon is high enough. Therefore,improving the conductivity of polycrystalline silicon layer with high doping level is beneficial to solar cell's performance.

References

[1] Cast P S, Padilla M, Kimmerle A and Reichel C 2014 *IEEE J. Photovolt.* **4** 114
[2] Kerschaver E V and Beaucarne G 2006 *Prog. Photovoltaics Res. Appl.* **14** 107
[3] Smith D D, Cousins P, Westerberg S, Tabajonda R D J, Aniero G and-Shen Y C 2014 *IEEE J. Photovolt.* **4** 1465
[4] Fong K C, Teng K, McIntosh K R, Blakers A W, Franklin E, Zin N and Fell A 2013 28*th EU-PVSEC*, 2013, Paris, France, p. 851
[5] O'Sullivan B J, Debucquoy M, Singh S, Castro A U D, Payo M R, Posthuma N E, Gordon I, Szlufcik J and Poortmans J 2013 28*th EU-PVSEC*, 2013, Paris, Frrance, p. 956
[6] Halm A, Mihailetchi V D, Galbiati G, Koduvelikulathu L J, Roescu R, Comparotto C, Kopecek R, Peter K and Libal J 2012 27*th EU-PVSEC*, 2012, Frankfurt, Germany, p. 20
[7] Masuko K, Shigematsu M, Hashiguchi T, Fujishima D, Kai M, Yoshimura N, Yamaguchi T, Ichihashi Y, Mishima T, Matsubara N, Yamanishi T, Takahama T, Taguchi M, Maruyama E and Okamoto S 2014 *IEEE J. Photovolt.* **4** 1433
[8] Krr M J and Cuevas A 2002 *Semicond. Sci. Technol.* **17** 35
[9] Aberle A G 2000 *Prog. Photovoltaics Res. Appl.* **8** 473
[10] Ingenito A, Isabella O and Zeman M 2015 *Prog. Photovoltaics Res. Appl.* **23** 1649
[11] Schmidt J and Kerr M 2001 *Sol. Energ. Mater. Sol. Cells* **65** 585
[12] Kerr M J, Schmidt J and Cuevas A 2001 *Appl. Phys. Lett.* **89** 3821
[13] Hoex B, Heil S B S, Langereis E, van de Sanden M C M and Kessels W M M 2006 *Appl. Phys. Lett.* **89** 042112
[14] Bonilla R S and Wilshaw P R 2014 *Appl. Phys. Lett.* **104** 232903
[15] Yang X, Múler R, Xu L J, Bi Q, Weber K, Franklin E and Benick J 2015 *IEEE J. Photovolt.* **5** 87
[16] Cesar I, Guillevin N, Burgers A R, Mewe A A, Bende E E, Rosca V, Aken B V, Koppes M, Anker J, Geerligs L J and Weeber A W 2014 29*th European Photovoltaic Solar Energy Conference and Exhibition*, 2014, Amsterdam, Netherlands, p. 633
[17] Roulston D J, Arora N D and Chamberlain S G 1982 *IEEE T. Electron Dev.* **29** 284
[18] Law M E, Solley E, Liang M and Burk D E 1991 *IEEE Electron Dev. Lett.* **12** 401
[19] Fossum J G and Lee D S 1982 *Solid State Electron.* **25** 741
[20] Slotboom J W and de Graaff H C 1976 *Solid State Electron* **19** 857